THE JOURNAL OF PHYSICAL CHEMISTRY B

ARTICLE

pubs.acs.org/JPCB

Is There a Liquid−Liquid Transition in Confined Water?

Limei Xu*,†,‡,§ and Valeria Molinero*,‡

†WPI-Advanced Institute for Materials Research, Tohoku University, 2-1-1 Katahira, Auba-ku, Sendai 980-8577, Japan

‡Department of Chemistry, University of Utah, 315 South 1400 East, Salt Lake City, Utah 84112-0850, United States

ABSTRACT: Water confined in narrow nanopores that prevent ice crystallization is usually studied as a means to understand the anomalous behavior of bulk liquid water. Nevertheless, there is no agreement on the similarity of the thermodynamics of bulk and nanoconfined liquid water. In this work, we use molecular dynamics simulations with the mW water model to investigate the phase behavior of liquid water in bulk and confined in a 1.5 nm cylindrical pore with water−surface interactions identical to water−water interactions. Through analysis of the isochors of bulk liquid water $V(T,p)$ we extrapolate the locus of a putative liquid−liquid critical point (LLCP) in bulk mW water at 190 K and 1215 atm. This is a "virtual LLCP", as it would lie in a region of the phase diagram where fast crystallization of water impedes equilibration of the liquid. We find that confinement has a weak effect on the loci of the thermodynamic anomalies: the maxima in density and heat capacity of confined water occur at T,p similar to that in bulk. The heat capacity peak of confined water is due to a transformation within the confined liquid; we verify that ice does not form in the pores. Confined mW water presents a heat capacity maximum $C_p^{max}(p)$ up to the highest pressure we investigated, 4000 atm. The magnitude of the heat capacity peak $C_p^{max}(p)$ has a nonmonotonous dependence with pressure, attaining a maximum at conditions close to those of the locus of the bulk water's virtual LLCP. We do not find, however, direct evidence of a first-order liquid−liquid transition in confined water for pressures above or below the locus of the maximum response function. The extreme value of the response functions of confined water could be a rounded manifestation of an equivalent feature in the free energy surface of bulk water.

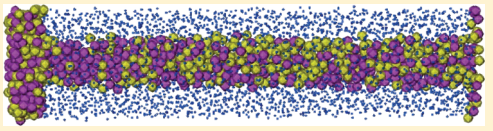

1. INTRODUCTION

Water is the most abundant liquid and a key solvent for biological systems. While ubiquitous, water exhibits many unusual properties, such as a density maximum and an increase of thermodynamic response functions (isobaric thermal expansion coefficient, isobaric specific heat, and isothermal compressibility) on cooling.[1−4] The origin of such unusual behavior of water has attracted extensive attention during the last decades, yet our understanding of the numerous thermodynamic anomalies of bulk water still remains incomplete. Different hypotheses[5−10] have been proposed to explain the anomalous thermodynamics of water. The most prominent of these theories is the liquid−liquid critical point (LLCP) hypothesis,[7] which postulates the existence of two liquid phases of water that would convert through a first-order transition terminating at a critical point located deep in the supercooled liquid region of water's phase diagram. Recent work by Mishima indicates that, if there is an LLCP, it would be located at $p_c \approx 500$ atm and $T_c \approx 223$ K.[11]

The experimental confirmation of the existence of the LLCP in bulk water remains an issue due to unavoidable crystallization in the region termed "no man's land", comprised between the temperature of homogeneous nucleation of ice, $T_H \approx 232$ K, and the glass transition temperature, $T_g \approx 136$ K.[10,12] Atomistic simulations have predicted the existence of an LLCP in bulk supercooled water[7,13−17] and water confined in 2.4 nm wide slit pores.[18] Recent simulation studies of the rate of ice crystallization using the mW coarse-grained model of water, however, indicate that for simulation cells that are much larger than the critical ice nucleus, bulk supercooled liquid water cannot be equilibrated in "no-man's land" because the time scale of ice nucleation is comparable to the time scale of relaxation of the liquid.[19,20] As the instability of the liquid results from its crystallization, the liquid state can only be studied down to very low temperatures through confinement of water in very narrow nanopores. Confinement lowers the melting temperature of ice, in a fashion well described by the Gibbs−Thomson equation.[21−23] The lowering of the melting temperature makes it possible to study the structural transformation of the cooled liquid in the stable state. It is not clear, however, whether a first-order liquid−liquid phase transition can occur in strongly confined water, as it approaches the case of a one-dimensional fluid.

Several studies have been performed to determine the liquid phase behavior of water confined in MCM-41 silica pores,[24−30] mostly with the goal of learning about the anomalous behavior of bulk water. Yet a direct comparison with bulk water is limited by the uncertainty of whether the behavior of an extremely confined liquid is qualitatively or quantitatively the same as the bulk one, and there is always the lingering question of whether the interaction of water with the pore-wall surface dominates the structure and phase behavior of water in nanopores.[31,32]

In this work we use molecular simulations with the mW water model to investigate the nature of the structural transformation

Special Issue: H. Eugene Stanley Festschrift

Received: May 30, 2011
Revised: July 22, 2011
Published: September 16, 2011

in liquid water confined in a narrow cylindrical nanopore that prevents the crystallization of ice. To separate the effect of confinement from that of the strength of the water−wall interaction, we study the phase behavior of water confined in a nanopore that interacts with water as water with itself. These simplified "water-pores" have already been used for the investigation of the crystallization of ice[21,33,34] and capillary condensation[35] in pores, where it was shown that they resemble in several properties the MCM-41 silica nanopores. Therefore, the pore of this study should provide a good model for comparison with the behavior of water in MCM-41 silica. The details of the model are presented in section 2. In section 3, we first estimate a locus for a putative LLCP in bulk mW water and then investigate the density, fraction of four-coordinated molecules, enthalpy, and heat capacity of water in 1.5 nm diameter "water-pores" as a function of temperature, for pressures up to 4000 atm. We address to what extent the thermodynamics of liquid water confined in this narrow nanopore is similar to that of bulk water, and, in particular, we investigate the structural evolution of liquid water at very low temperatures in the confined system and assess whether there is a first-order liquid−liquid transition in confined water when crystallization does not intervene.

2. MODELS AND METHODS

Bulk and confined water were simulated with the computationally efficient coarse-grained monatomic water model mW,[36] in which each water molecule is represented by a single particle interacting through a nonisotropic potential that mimics hydrogen bonds. The mW model has no hydrogen atoms or electrostatics, yet it reproduces the structure, anomalies, and phase transitions of water.[19,21,36−38] As observed in the experiment, the structural transformation toward a low-density liquid in supercooled liquid mW competes with ice nucleation.[19−21,36,37]

The simulation cells of water-filled 1.5 nm diameter nanopores are built following the protocols of ref 21: we first equilibrate a block of liquid water with 4096 molecules and approximate dimensions $L_x = L_y = 30$ Å and $L_z = 130$ Å using isobaric and isothermal molecular dynamics simulation at $T = 300$ K and a target pressure p. We then define two regions: the liquid and the nanopore wall. The liquid comprises the region within a nanopore with radius $R = 7.5$ Å from the center of the water block along the z-axis, plus a 10 Å wide slab at one end of the cell to act as buffer to compensate the volume change under constant pressure simulations. The rest of the water block is assigned as the nanopore wall. The water molecules within the nanopore wall are bonded to their first neighbors (within 3.5 Å) through harmonic bonds that restrain the molecules around their positions in the 300 K configuration from which the pore is made, with a bond constant $k = 100$ kcal/mol Å^2. The bonds keep the nanopore−wall structure from undergoing a structural transformation or breaking upon volume expansion or contraction. The water−wall interaction is the same as the water−water interactions, as described in ref 36.

The phase behavior of bulk water was investigated using a periodic simulation cell containing 8192 mW water particles. We performed equilibration runs for times up to 50 ns for temperatures down to around 200 K along each isochore with number density in the range 0.031−0.037. Lower temperatures resulted in the spontaneous crystallization of ice during the equilibration time; simulations for which ice crystallization occurred were discarded. The isochors were fitted with fifth-order polynomial,[39] with which they were extrapolated into the region where fast crystallization of ice prevents the equilibration of liquid water.

Molecular dynamics simulations were performed using LAMMPS.[40,41] The equations of motion were integrated with the velocity verlet algorithm with 5 fs time steps. Water in the nanopore was simulated in the constant temperature and pressure (NpT) ensemble and bulk water in the constant temperature and volume (NVT) ensemble. T and p were controlled with a Nose−Hoover thermostat and barostat with relaxation times of 1 and 5 ps, respectively. We collected data for the nanopore at a series of state points with pressures ranging from 500 to 4000 atms. For each pressure, the temperature was decreased in a stepwise ramp, starting at 300 K and decreasing 5 K every 60 ns. At T of about 200 K, the root-mean-square displacement in the z direction (the pore axis) during 60 ns is more than twice the length of the pore.

To compute the density of water confined in the nanopore, we subtracted from the total volume of the cell, V_{total}, the volume V_{wall} occupied by the N_{wall} molecules of the pore wall under the same thermodynamic conditions. To this end, we performed additional simulations at each state point of a block with the same dimensions of the one used to construct the pore plus confined water system, but in which all the particles were connected through harmonic bonds to mimic a block of pore wall material in the original configuration at 300 K and pressure p. From these simulations we determined the temperature evolution of the volume of the wall, V_{wall}, which decreases monotonously on cooling. The volume per molecule of confined water was computed as $V_{water} = (V_{total} - V_{wall}N_{wall}/(N_{wall} + N_{water}))/N_{water}$, where N_{water} is the number of water molecules in the pore. The enthalpy of the confined water was calculated as $H = U + pV$, where U and V are the average energy and volume per molecule of confined water. U includes the water−water and water−surface interactions, but does not include interactions between particles in the pore wall. The heat capacity of confined water was obtained as the finite difference derivative of the enthalpy of confined water with respect to the temperature.

3. RESULTS AND DISCUSSION

Water crystallizes easily on cooling experiments. This is also the case for mW water.[19,20] At room pressure, the crystallization rate of mW water is the fastest at $T_x \approx 200$ K.[20] Crystallization of bulk mW water can be avoided by fast cooling of the liquid, a process that yields low-density amorphous ice (LDA).[36,37] Almost all the water molecules in LDA are already four-coordinated (as in ice) although they lack the long-range structure of the crystal.[37] The structural transformation toward a four-coordinated structure on fast cooling is continuous but sharp, and values of properties associated with structural change (the change in the fraction of four-coordinated molecules, tetrahedral order and the density, and the value of the constant pressure heat capacity) peak at the liquid transformation temperature $T_L = 202 \pm 2$ K, almost identical to T_x. Below that temperature, supercooled liquid water cannot be equilibrated because the time for nucleation of ice is comparable to or shorter than the time for equilibration of the liquid: bulk liquid water reaches a lower limit of metastability around T_L.[19,20]

The extrapolation of the isochors of mW liquid water and into the deeply supercooled region (Figure 1) suggests a locus of divergent compressibility around 190 K and 1215 atm. This would suggest the existence of a LLCP in bulk mW water at that location. Nevertheless, we find that this region and all the putative

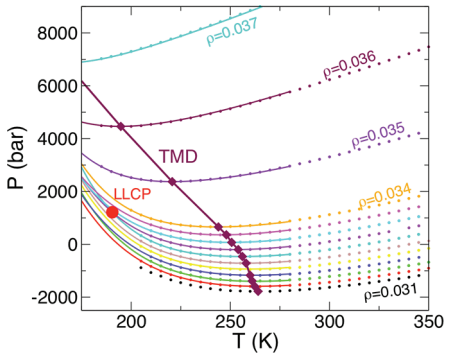

Figure 1. Phase behavior of bulk liquid water. The temperature and pressure dependence of the isochors of bulk mW water (dots) and their extrapolation into their deeply supercooled region (thin lines) suggest the existence of a locus of diverging compressibility at 190 K and 1215 atm (red circle). This locus could be a virtual LLCP, as it is located in a region of the phase diagram where supercooled bulk liquid crystallizes before it can be equilibrated. The dots indicate the averages of p over simulations at constant number density ρ and temperature T; the lines are extrapolations of these data sets with fifth-order polynomials, as in ref 39. The thick maroon line runs through the loci of density maxima (equivalent to pressure minima on the isochors, shown as diamonds).

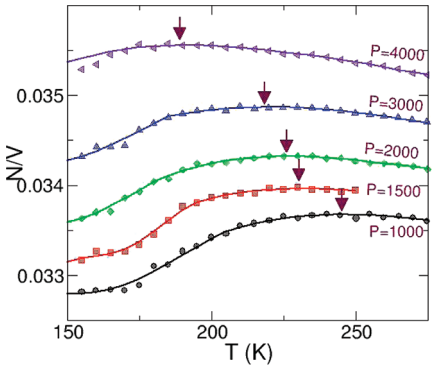

Figure 2. Density of nanoconfined water. mW water confined in 1.5 nm diameter nanopores presents well-defined density maxima up to the highest pressure of this study, 4000 atm. The symbols show the density $\rho = N/V$ along each isobar. The lines are guides to the eye, and the arrows indicate the loci of maximum density obtained by polynomial fitting near the density maximum along each pressure.

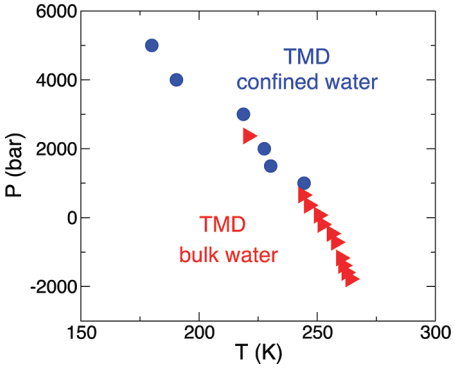

Figure 3. Density anomaly of bulk and confined water. The TMD for confined water (blue circles) and bulk water (red triangles) decrease with pressure and are within a few degrees of each other, in agreement with the experimental reports of refs 25 and 26.

liquid−liquid line cannot be accessed in equilibrium simulations, as crystallization occurs too fast for the equilibration of the tetrahedrally coordinated liquid. We note that the LLCP of the ST2 and TIP4P/2005 models have been computed in simulations without any observation of crystallization using simulation cells with ∼500 molecules.[13,16] The lack of crystallization in those systems is probably due to their small size, as it is known that the nucleation rate is the lowest for systems with dimensions comparable to the critical nucleus, which for ice is about 100 molecules.[20] Our projection of a virtual LLCP in a region just below a lower limit of metastability of water is consistent with Kiselev's predictions using the relaxation theory of metastable states[42] and the very recent Bertrand and Anisimov's scaling-theory equation of state analysis of the thermodynamics of water.[43] Recent umbrella sampling free energy maps computed for the mW and ST2 models as a function of density and the global bond order parameter Q_6 do not evidence signatures of an LLCP in the free energy landscape of these models of water.[44]

We now turn our focus to the phase behavior of liquid water confined in the 1.5 nm nanopores. The nanopore of this study is a good model[21,35] for the 1.5 nm diameter MCM-41 silica pores used as in the experiments of refs 24−29. Confinement of water in cylindrical nanopores depresses the melting temperature of ice. The depression of the melting temperature with respect to the bulk value, ΔT_m, is usually well represented by the modified Gibbs−Thomson equation, $\Delta T_m = K_{GT}/(R - d)$,[21−23,45] where R is the radius of the pore and $d \approx 0.5$ nm is the width of the premelted liquid layer between the ice core and the pore wall. K_{GT} is the Gibbs−Thomson constant, with a value of 52 K·nm in experiments[22] and 54 K·nm for mW water.[21,45] This equation suggests that the melting point for ice in a nanopore of radius R = 0.75 nm would be lower than the glass transition temperature for water, $T_g \approx$140 K. Elsewhere is shown that mW water confined in narrow nanopores with diameter 2 nm or lower does not nucleate ice,[45] in agreement with the experiments.[22,23,46,47]

The confined liquid water displays a maximum in the density as a function of temperature for the entire range of pressures analyzed (Figure 2). The existence of a temperature of maximum density (TMD) was previously reported from experimental studies of confined water in silica pores.[25,26] The TMD determined in these studies is essentially the same as that for bulk water.[25,26] The density maximum of confined water in the simulations moves to lower temperatures with increase in pressure (Figure 3). The simulations suggest that confinement itself (i.e., by a wall that interacts with water in the same way as water with itself) does not significantly affect the locus of the density anomaly in water: the TMDs of confined and bulk water in Figure 3 are within a few degrees. Zhang et al. have studied the density ρ of heavy confined water in MCM-41 silica pores with the same diameter as in the present study as a function of pressure and temperature, through the study of the intensity of the Bragg peak they obtained from neutron scattering of the samples.[29] These authors report the existence of a kink in $\rho(T)$ for low pressures, and loss of the kink and development of hysteresis on the cooling and heating cycles at higher pressures. They interpret this as indicative of the existence of a tricritical point in confined water.[29] A kink in $\rho(T)$ along the Widom line (the supercritical continuation of a liquid−liquid first order line[8]) was previously reported for the mean field analysis of the phase behavior of a bulk water-like lattice model.[48]

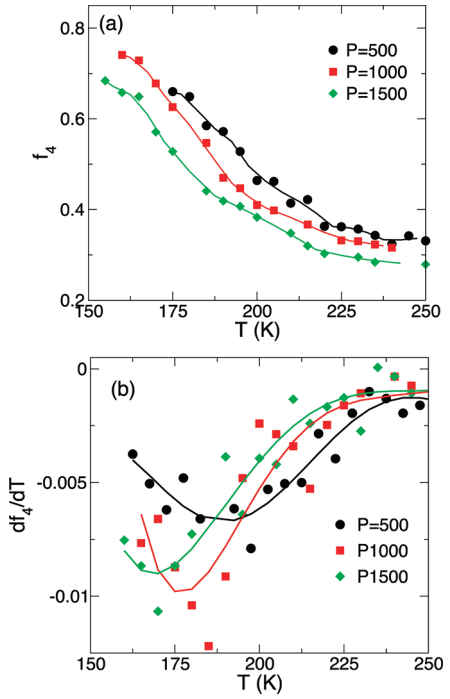

Figure 4. Structural changes in confined water on cooling along isobars. (a) Fraction of four-coordinated water molecules, f_4, upon cooling along three isobars. (b) Derivative of the fraction of four-coordinated molecules with respect to the temperature, df_4/dT, along these same isobars was computed through finite difference of $f_4(T)$; the solid line shows the best second-order polynomial fit to df_4/dT. The structural response function, although noisy, shows a well-defined maximum $(df_4/dT)^{MAX}$ for each pressure. The maximum in $(df_4/dT)^{MAX}$ occurs at p_{MAX} around 1000 atm.

The kink in the density is not observed in other experimental studies of nanoconfined water. We observe a change of slope in density as a function of temperature yet no diverging behavior is seen in the derivative of the density as a function of temperature within the pressure range of our study.

The decrease in density of the confined liquid is accompanied by a change in the local structure of water that involves an increase in tetrahedral order and in the fraction of four-coordinated molecules.[37] The fraction of four-coordinated molecules (defined as the average number of water molecules with exactly four neighbors within the first peak of the radial distribution function, 3.5 Å) increases upon cooling along the isobars and decreases upon compression along isotherms (Figure 4a). The derivative of the fraction of four-coordinated molecules, df_4/dT (Figure 4b) is a measure of the sharpness of the structural change in the confined water. The structural response function df_4/dT at each pressure presents a maximum $(df_4/dT)^{MAX}$ that moves to lower temperatures on compression, following the same trend as the TMD with pressure. The magnitude of the peak in the structural response function $(df_4/dT)^{MAX}$ has a non-monotonous dependence on pressure: its maximum occurs at $p_{MAX} \approx 1000$ atm. Interestingly, this pressure is quite close to the one of the virtual (unattainable) LLCP obtained by extrapolation of the isochores of bulk mW water, 1215 atm (Figure 1). We note, however, that the structural transformation seems to be continuous for the entire pressure range studied, above and below the pressure of the maximum structural response function p_{MAX}. A discontinuous transformation may seem continuous due to the finite response time and

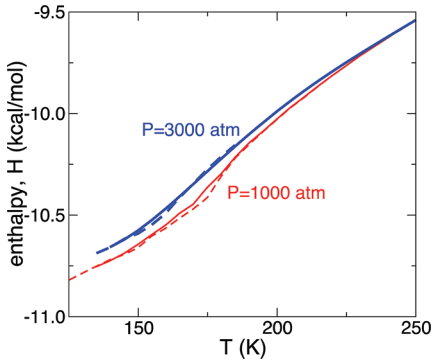

Figure 5. Enthalpy of confined water as a function of temperature. The enthalpy is presented for the pressure of maximum response function, p_{MAX} = 1000 atm (red lines) and well above that pressure, 3000 atm. Cooling (solid lines) and heating (dashed lines) cycles are shown. There is negligible hysteresis between the cooling and heating cycles, and the hysteresis does not become more pronounced at high pressures, as would be expected if a first-order transition between two liquid phases with a with a LLCP with pressure around 1000 atm (the locus of maximum structural response and maximum heat capacity peaks) occurred in confined liquid water.

finite length of the simulation cell; therefore we investigate the hysteresis on cooling and heating to assess whether the structural transformation in confined water could be first order.

Hysteresis on cooling and heating is characteristic of most first-order transitions. The enthalpy of the confined water does not present any significant hysteresis, even at pressures above p_{MAX} (Figure 5), suggesting the absence of a first-order liquid−liquid transition in the nanoconfined water. We do not observe two well-defined liquid phases (if we assume the low-density liquid to be mostly four-coordinated, as LDA[37]) in coexistence under any condition, but rather one liquid phase with fluctuating domains of four-coordinated water molecules and domains of water molecules with higher number of neighbors in their first solvation shell (see the abstract figure). We note that approaching the liquid transformation temperature T_L = 202 K, room pressure bulk mW water develops patches of four-coordinated liquid with characteristic dimensions larger than the diameter of the present nanopore; therefore confinement of water will dampen these fluctuations and their growth on cooling, affecting the magnitude of response functions, such as the structural response df_4/dT, the compressibility, and the heat capacity.

The heat capacity $C_p = dH/dT$ of the confined water presents distinct peaks that move to lower temperatures on compression (Figure 6a). The maximum in the heat capacity coincides with the maximum structural change and the maximum change in density, as has been previously reported for bulk models of water and other tetrahedrally coordinated liquids.[16,20,37,49,50] Johari has suggested that the heat capacity peak obtained for water confined in a 1.8 nm silica pore is due to the formation of cubic ice with stacking faults.[51] The mW model correctly describes the melting and formation of ice in nanopores, predicting the formation of cubic ice with profuse hexagonal stacking faults,[21,33] as suggested by X-ray diffraction experiments.[52] We verified, using the CHILL algorithm,[21] that no ice formed within the 1.5 nm diameter pores at any of the conditions of this study; the heat capacity peak is entirely due to a process within the liquid phase: the structural transformation into a four-coordinated liquid.

The temperature T^{max} of the heat capacity peak, C_p^{max}, of the confined water is very close to that found for bulk water with the

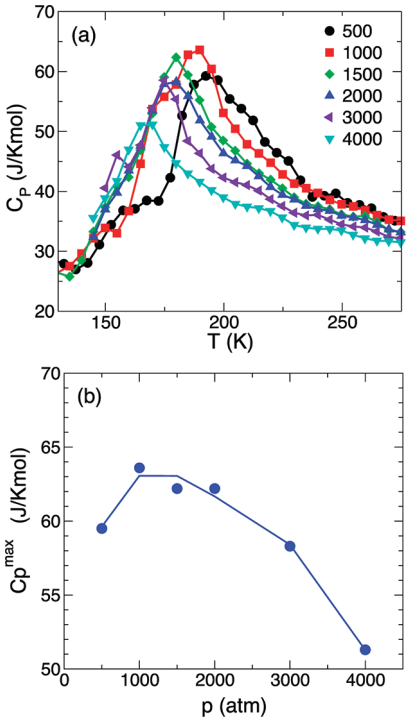

Figure 6. Heat capacity of water confined in the 1.5 nm diameter nanopores. (a) The capacity, C_p, versus temperature along isobars present clear maxima, with peaks that move to lower temperatures on compression. (b) The maximum value of the heat capacity for each pressure, C_p^{max}, has a nonmonotonous dependence with pressure. The maximum response is observed at $p_{MAX} \approx 1000$ atm.

mW model: the C_p^{max} of bulk water at 1 atm occurs at 202 K[20] and the C_p^{max} of nanoconfined water at 500 atm occurs at 192 K. This indicates that confinement in a pore with water−wall interactions equivalent to water−water interactions has a weak effect on the loci of water anomalies, in significant contrast to the displacement of the liquid−ice equilibrium. Our results agree with those of Nagoe et al., who used DSC to determine the heat capacity of water confined in MCM-41 silica pores and found that confined water has a heat capacity peak at temperature T^{max} that has very weak dependence on pore size in the range of diameters 2.3−1.7 nm, conditions in which crystallization of ice does not interfere.[30] Theoretical predictions of the heat capacity of confined water concur with this conclusion.[43]

While the T^{max} is quite insensitive to confinement, experiments and theory indicate that the magnitude of C_p^{max} decreases as water is confined in narrower pores.[30,43] A comparison between the value of the peak of the heat capacity for bulk and confined water shows the same effect in the simulations: the heat capacity of bulk mW water at 1 atm reaches a maximum of 102 J/K·mol at 202 K;[20] this corresponds to an increase of 62 J/K·mol from its value at 250 K. The heat capacity of water confined in the 1.5 nm pore at 500 atm reaches a maximum of 60 J/K·mol at 192 K, just 21 J/K·mol higher than the C_p of the confined water at 250 K at that pressure. The increase in C_p for the confined water predicted by the simulations is comparable to the one measured by DSC, between 10 and 20 J/K·mol.[30] The lower increase in heat capacity in confined water reflects a more rounded structural transformation in the nanopore than in bulk.

The loss of sharpness is probably due to the dampening of structural fluctuations (associated with energy fluctuations) as the width of the pore has dimensions comparable to the correlation length of bulk water a few degrees above T_L.[37] The water molecules at the pore wall, in contact with a wall that has the structure of liquid water at 300 K, are more reluctant to acquire four-coordination: the fraction of four-coordinated molecules for the confined water is less than 0.8 at 160 K (Figure 4a), while it is about 0.9 for bulk water at that temperature.[37] Reduction of the response functions was observed in simulations of a water-like lattice model confined in a nanoslit when particles that encouraged a certain ordering of the liquid were randomly placed within the slit.[53] We note that the nanopores of this work are much shorter than the typical silica pores used in experiments, which are usually micrometers long. As the pores of this study contain a non-negligible fraction of the water in the ∼1 nm long "bulk-like" slab designed to accommodate the volume change of water with temperature, we expect that for a micrometer sized pore, the density anomaly is slightly more displaced toward lower temperatures, and the response functions are even more depressed than for the ∼12 nm long pore of this work.

T^{max} moves to lower pressures on compression: T^{max} at 4000 atm is 25 K lower than at 500 atm. More interestingly, the height of the C_p^{max} also changes with pressure, presenting a maximum around $p_{MAX} \approx 1000$ atm (Figure 6b), the same pressure at which the structural response function df_4/dT reaches its maximum value. It is interesting that the loci of maximum in the reponse functions of the confined water occur at conditions that are roughly the same as the extrapolated LLCP in bulk water. The bulk LLCP of mW cannot be attained because it is below the limit of metastability of the supercooled liquid; nevertheless it seems to strongly affect the thermodynamics of liquid water above the line of homogeneous nucleation of ice. In the case of water confined in a 1.5 nm diameter pore, the crystallization can be avoided, and the liquid undergoes the structural transformation in the stable region (above the melting point of the confined ice). The transformation, however, does not seem to be first order, even at pressures above the maximum of the response functions, which could be interpreted as the "shadow" of the extrapolated unattainable LLCP for bulk water.

4. CONCLUSIONS

The isochors of bulk liquid water modeled with the mW model point to a locus of maximum compressibility around 190 K and 1215 atm. This would suggest the existence of an LLCP in bulk mW water at that state point, but fast crystallization makes it impossible to equilibrate liquid water around and below the temperatures of the liquid transformation: the structural transformation of the liquid phase cannot be disentangled from the formation of ice in bulk supercooled water, at least for simulation cells much larger than the size of the critical ice nuclei.

Ice crystallization can be avoided by confining the liquid in narrow nanopores that depress the melting temperature to values below those of the structural transformation of the liquid phase. We used this approach to investigate the thermodynamics and phase behavior of water confined in a 1.5 nm diameter nanopore with water−wall interactions identical to those that water has with water. Previous studies of capillary condensation and ice crystallization indicate that these pores are a good approximation for MCM-41 silica pores.[21,35]

Confinement is known to smear first-order transitions, thus even well-defined first-order transitions in bulk, e.g. the liquid−ice or liquid−vapor equilibria, appear rounded and would not be

first-order in nanoconfinement.[54,55] In our study with the mW water model, the confined liquid water undergoes a sharp but continuous structural transformation to a mostly four-coordinated amorphous phase at all the pressures of this study. We note, however, that lack of a first-order transition in nanoconfined water is not sufficient to rule out the existence of a liquid−liquid transition in the bulk fluid. We note, however, that simulations with the mW model produce ice crystallization in narrow nanopores, down to 1.25 nm radius.[21,33,45] As the structural gap between liquid and ice is larger than the one expected for two distinct liquid phases of water and crystallization of water in nanopores is observed for mW water in pores wider than 2.5 nm diameter,[21,33,34,45] the results of this work suggest that the lack of evidence of a first-order transition in the simulations at high pressures is not due to slow kinetics but to a genuine absence of a discontinuous liquid−liquid transition for water confined in the 1.5 nm diameter pore of this study.

AUTHOR INFORMATION

Corresponding Author

*E-mail: limei.xu@pku.edu.cn (L.X.); Valeria.Molinero@utah.edu (V.M.).

Present Addresses

[§]International Center for Quantum Materials, Peking University, Beijing 100871, China.

ACKNOWLEDGMENT

We thank Sergey V. Buldyrev and Pablo G. Debenedetti for helpful discussions. This work was supported by a Seed Grant by the University of Utah and the Arnold and Mabel Beckman Foundation through their Young Investigator Program (V.M.), and the World Premier International Research Center Initiative (WPI initiative, Japan), as well as Grant-in-Aid for young scientists (L.X.). We acknowledge allocation of computing time by the Center of High Performance Computing of the University of Utah and the advanced Fluid Information Research Center of the Institute of Fluid Science at Tohoku University.

REFERENCES

(1) Angell, C. A.; Shuppert, J.; Tucker, J. C. *J. Phys. Chem.* **1973**, *77*, 3092.
(2) Angell, C. A.; Kanno, H. *Science* **1976**, *193*, 1121.
(3) Debenedetti, P. G. *J. Phys.: Condens. Matter* **2003**, *15*, R1669.
(4) Debenedetti, P. G.; Stanley, H. E. *Phys. Today* **2003**, *56*, 40.
(5) Sastry, S.; Debenedetti, P. G.; Sciortino, F. *Phys. Rev. B* **1996**, *53*, 6144.
(6) Speedy, R. J. *J. Phys. Chem.* **1982**, *86*, 982.
(7) Poole, P. H.; Sciortino, F.; Essmann, U.; Stanley, H. E. *Nature* **1992**, *360*, 324.
(8) Xu, L. M.; Kumar, P.; Buldyrev, S. V.; Chen, S. H.; Poole, P. H.; Sciortino, F.; Stanley, H. E. *Proc. Natl. Acad. Sci. U.S.A.* **2005**, *102*, 16558.
(9) Mishima, O.; Stanley, H. E. *Nature* **1998**, *396*, 329.
(10) Angell, C. A. *Science* **2008**, *319*, 582.
(11) Mishima, O. *J. Chem. Phys.* **2010**, *133*, 144503.
(12) Mishima, O. *Nature* **1996**, *384*, 546.
(13) Liu, Y.; Panagiotopoulos, A. Z.; Debenedetti, P. G. *J. Chem. Phys.* **2009**, *131*, 104508.
(14) Yamada, M.; Mossa, S.; Stanley, H.; Sciortino, F. *Phys. Rev. Lett.* **2002**, *88*, 195701.
(15) Paschek, D. *Phys. Rev. Lett.* **2005**, *94*, 217802.
(16) Abascal, J. L. F.; Vega, C. *J. Chem. Phys.* **2010**, *133*, 234502.
(17) Brovchenko, I.; Geiger, A.; Oleinikova, A. *J. Chem. Phys.* **2005**, *123*, 044515.
(18) Brovchenko, I.; Oleinikova, A. *J. Chem. Phys.* **2007**, *126*, 214701.
(19) Moore, E. B.; Molinero, V. *J. Chem. Phys.* **2010**, *132*, 244504.
(20) Moore, E. B., Molinero, V. Structural transformation in water controls the crystallization rate of ice *Nature* **2011**, accepted for publication; arXiv:1107.1622v1 [cond-mat.soft].
(21) Moore, E. B.; de la Llave, E.; Welke, K.; Scherlis, D. A.; Molinero, V. *Phys. Chem. Chem. Phys.* **2010**, *12*, 4124.
(22) Jahnert, S.; Chavez, F. V.; Schaumann, G. E.; Schreiber, A.; Schonhoff, M.; Findenegg, G. H. *Phys. Chem. Chem. Phys.* **2008**, *10*, 6039.
(23) Schreiber, A.; Ketelsen, I.; Findenegg, G. H. *Phys. Chem. Chem. Phys.* **2001**, *3*, 1185.
(24) Liu, L.; Chen, S.-H.; Faraone, A.; Yen, C.-W.; Mou, C.-Y. *Phys. Rev. Lett.* **2005**, *95*, 4.
(25) Liu, D. Z.; Zhang, Y.; Chen, C. C.; Mou, C. Y.; Poole, P. H.; Chen, S. H. *Proc. Natl. Acad. Sci. U.S.A.* **2007**, *104*, 9570.
(26) Mallamace, F.; Branca, C.; Broccio, M.; Corsaro, C.; Mou, C. Y.; Chen, S. H. *Proc. Natl. Acad. Sci. U.S.A.* **2007**, *104*, 18387.
(27) Mallamace, F.; Broccio, M.; Corsaro, C.; Faraone, A.; Majolino, D.; Venuti, V.; Liu, L.; Mou, C. Y.; Chen, S. H. *Proc. Natl. Acad. Sci. U.S.A.* **2007**, *104*, 424.
(28) Mallamace, F.; Corsaro, C.; Broccio, M.; Branca, C.; Gonzalez-Segredo, N.; Spooren, J.; Chen, S. H.; Stanley, H. E. *Proc. Natl. Acad. Sci. U.S.A.* **2008**, *105*, 12725.
(29) Zhang, Y.; Faraone, A.; Kamitakahara, W. A.; Liu, K.-H.; Mou, C.-Y.; Leão, J. B.; Chang, S.; Chen, S.-H. arXiv:1005.5387v3 [cond-mat.soft], 2010.
(30) Nagoe, A.; Kanke, Y.; Oguni, M.; Namba, S. *J. Phys. Chem. B* **2010**, *114*, 13940.
(31) Soper, A. *Molecular Physics, 106* **2008**, *16*, 2053.
(32) Ricci, M. A.; Bruni, F.; Giuliani, A. *Faraday Discuss* **2008**, *141*, 347.
(33) Gonzalez Solveyra, E.; De La Llave, E.; Scherlis, D. A.; Molinero, V. Melting and crystallization of ice in partially filled nanopores. *J. Phys. Chem. B.* **2011**, DOI: 10.1021/jp205008w.
(34) Moore, E. B.; Allen, J. T.; Molinero, V. Liquid−ice coexistence below the melting temperature for water confined in hydrophilic and hydrophobic nanopores. To be submitted for publication.
(35) De La Llave, E.; Molinero, V.; Scherlis, D. A. *J. Chem. Phys.* **2010**, *133*, 034513.
(36) Molinero, V.; Moore, E. B. *J. Phys. Chem. B* **2009**, *113*, 4008.
(37) Moore, E. B.; Molinero, V. *J. Chem. Phys.* **2009**, *130*, 244505.
(38) Jacobson, L. C.; Hujo, W.; Molinero, V. *J. Phys. Chem. B* **2009**, *113*, 10298.
(39) Poole, P. H.; Saika-Voivod, I.; Sciortino, F. *J. Phys.: Condens. Matter* **2005**, *17*, L431.
(40) Plimpton, S. J. *J. Comput. Phys.* **1995**, *117*, 1.
(41) Plimpton, S. J. Available online at lammps.sandia.gov, 2005.
(42) Kiselev, S. *Int. J. Thermophys.* **2001**, *22*, 1421.
(43) Bertrand, C. E.; Anisimov, M. A. *J. Phys. Chem. B* **2011**, DOI: dx.doi.org/10.1021/jp204011z.
(44) Limmer, D.; Chandler, D. arXiv:1107.0337v1 [cond-mat.stat-mech], 2011.
(45) de la Llave, E.; Gonzalez Solveyra, E.; Scherlis, D. A.; Molinero, V. in preparation, 2011.
(46) Kittaka, S.; Ishimaru, S.; Kuranishi, M.; Matsuda, T.; Yamaguchi, T. *Phys. Chem. Chem. Phys.* **2006**, *8*, 3223.
(47) Morishige, K.; Kawano, K. *J. Chem. Phys.* **1999**, *110*, 4867.
(48) Franzese, G.; Stanley, H. E. *J. Phys.: Condens. Matter* **2007**, *19*, 205126.
(49) Kumar, P.; Franzese, G.; Stanley, H. E. *Phys. Rev. Lett.* **2008**, *100*, 105701.
(50) Hujo, W.; Jabes, B. S.; Rana, V. K.; Chakravarty, C.; Molinero, V. The rise and fall of anomalies in tetrahedral liquids. *J. Stat. Phys.* **2011**, DOI: 10.1007/s10955-011-0293-9.
(51) Johari, G. P. *J. Chem. Phys.* **2009**, *130*, 124518.
(52) Morishige, K.; Uematsu, H. *J. Chem. Phys.* **2005**, *122*, 044711.

(53) Strekalova, E.; Mazza, M.; Stanley, H.; Franzese, G. *Phys. Rev. Lett.* **2011**, *106*, 145701.
(54) Winkler, A.; Wilms, D.; Virnau, P.; Binder, K. *J. Chem. Phys.* **2010**, *133*, 164702.
(55) Tarazona, P.; Marconi, U. M.; Evans, R. *Mol. Phys.* **1987**, *60*, 573.